

# Molding Block Copolymer Micelles: A Framework for Molding of Discrete Objects on Surfaces

Sherryl Y. Yu-Su,<sup>†</sup> David R. Thomas,<sup>†,‡</sup> Jonathan E. Alford,<sup>§,||</sup> Isaac LaRue,<sup>†,⊥</sup> Marinos Pitsikalis,<sup>#</sup> Nikos Hadjichristidis,<sup>#</sup> Joseph M. DeSimone,<sup>†</sup> Andrey V. Dobrynin,<sup>∇</sup> and Sergei S. Sheiko<sup>\*,†</sup>

Department of Chemistry, Caudill and Kenan Laboratories, The University of North Carolina at Chapel Hill, Chapel Hill, North Carolina 27599, Mechanical and Chemical Engineering Department, North Carolina A&T State University, Greensboro, North Carolina 27411, Department of Chemistry, University of Athens, Panepistimiopolis Zographou 15771 Athens, Greece, and Institute of Materials Science, University of Connecticut, Storrs, Connecticut 06269-3136

Received August 7, 2008. Revised Manuscript Received September 6, 2008

Soft lithography based on photocurable perfluoropolyether (PFPE) was used to mold and replicate poly(styrene-*b*-isoprene) block-copolymer micelles within a broad range of shapes and sizes including spheres, cylinders, and torroids. These physically assembled nanoparticles were first formed in a selective solvent for one block then deposited onto substrates having various surface energies in an effort to minimize the deformation of the micelles due to attractive surface forces. The successful molding of these delicate nanoparticles underscores two advantages of PFPE as a molding material. First, it allows one to minimize particle deformation due to adsorption by using low energy substrates. Second, PFPE is not miscible with the organic micelles and thus prevents their dissociation. For spherical PS-*b*-PI micelles, a threshold value of the substrate surface energy for the mold to lift-off cleanly, that is, the particles remain adhered to the substrate after mold removal was determined to be around  $\gamma \cong 54$  mJ/m<sup>2</sup>. For substrates with higher surface energies (>54 mJ/m<sup>2</sup>), the micelles undergo flattening which increase the contact area and thus facilitate molding, although at the expense of particle deformation. The results are consistent with theoretical predictions of a molding range for substrate surface energies, which depends on the size, shape, and mechanical properties of the particles. In a similar fashion, cylindrical PS-*b*-PI micelles remain on the substrate at surface energies  $\gamma \geq 54$  mJ/m<sup>2</sup> after a mold removal. However, cylindrical micelles behaved differently at lower surface energies. These micelles ruptured due to their inability to slide on the surfaces during mold lift-off. Thus, the successful molding of extended objects is attainable only when the particle is adsorbed on higher energy substrates where deformation can still be kept at a minimum by using stronger materials such as carbon nanotubes for the master.

## Introduction

Soft lithography is a popular and facile approach to nanofabrication,<sup>1–4</sup> which effectively eases the limitations in sizes and structures available for replication when compared to conventional photolithographic techniques where replication is restricted to planar surfaces, simple geometries, and conventional materials.<sup>3</sup> In soft lithography, a master, typically made by photolithography, is molded and replicated using an elastomeric material. Currently, polydimethyl siloxane (PDMS) is the standard elastomer used, as there are many advantages to using it which include ease of fabrication, durability, optical transparency, gas-permeability, and favorable mechanical properties, that is, strength and flexibility.<sup>1–4</sup> However, the solubility of PDMS in organic

solvents and its relatively high adhesion limit its applicability.<sup>1–6</sup> Recently, DeSimone et al. developed a nanofabrication procedure using photocurable perfluoropolyether (PFPE), which has the desirable mechanical properties of PDMS but, in addition, has better solvent resistance and a lower surface energy ( $\gamma \cong 12–16$  mJ/m<sup>2</sup>) than PDMS ( $\gamma \cong 23$  mJ/m<sup>2</sup>).<sup>7–9</sup> Using homemade<sup>7–9</sup> as well as commercially available<sup>10</sup> PFPE, sub-100 nm size features have been successfully replicated with high fidelity from solid masters, as well as scum-free particles that are compatible with a variety of materials including biological agents.<sup>8–11</sup>

In addition to traditional solid masters, the low adhesion properties of PFPE allows for the molding and replication of weakly adsorbed nanoparticles with sizes ranging from 1 to 50 nm. Most importantly, PFPE enables molding of soft and fragile assemblies of organic molecules, such as viruses and micelles, which require special molecules and thermodynamic conditions to form and maintain their structures. This is a significant advantage, because it provides an opportunity to mold and

\* To whom correspondence should be addressed. E-mail: sergei@email.unc.edu.

<sup>†</sup> The University of North Carolina at Chapel Hill.

<sup>‡</sup> Current address: Department of Chemistry, University of Utah, Salt Lake City, UT 84112.

<sup>§</sup> North Carolina A&T State University.

<sup>||</sup> Current address: Exxon Mobil, Baton Rouge, LA.

<sup>#</sup> Current address: Department of Chemistry, King's College, Wilkes-Barre, PA 18711.

<sup>∇</sup> University of Athens.

<sup>⊥</sup> University of Connecticut.

(1) Zhao, X. M.; Xia, Y.; Whitesides, G. M. *J. Mater. Chem.* **1997**, *7*, 1069–1074.

(2) Xia, Y.; Whitesides, G. M. *Annu. Rev. Mater. Sci.* **1998**, *28*, 153–184.

(3) Gates, B. D.; Xu, Q.; Stewart, M.; Ryan, D.; Wilson, C. G.; Whitesides, G. M. *Chem. Rev.* **2005**, *105*, 1171–1196.

(4) Gates, B. D. *Mater. Today* **2005**, *8*, 44–49.

(5) Quist, A. P.; Pavlovic, E.; Oscarsson, S. *Anal. Bioanal. Chem.* **2005**, *381*, 591–600.

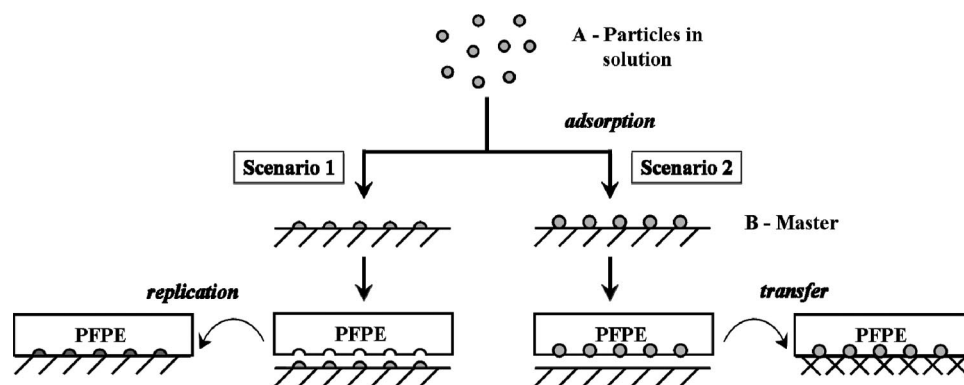
(6) Lee, J. N.; Park, C.; Whitesides, G. M. *Anal. Chem.* **2003**, *75*, 6544–6554.  
(7) Rolland, J. P.; Dam, R. M. V.; Schorzman, D. A.; Quake, S. R.; DeSimone, J. M. *J. Am. Chem. Soc.* **2004**, *126*, 2322–2323.

(8) Rolland, J. P.; Hagberg, E. C.; Denison, G. M.; Carter, K. R.; DeSimone, J. M. *Angew. Chem., Int. Ed.* **2004**, *43*, 5796–5799.

(9) Rolland, J. P.; Maynor, B. W.; Euliss, L. E.; Exner, A. E.; Denison, G. M.; DeSimone, J. M. *J. Am. Chem. Soc.* **2005**, *127*, 10096–10100.

(10) Truong, T. T.; Lin, R.; Jeon, S.; Lee, H. H.; Maria, J.; Gaur, A.; Hua, F.; Meinel, I.; Rogers, J. A. *Langmuir* **2007**, *23*, 2898–2905.

(11) Maynor, B. W.; Euliss, L. E.; Rolland, J. P.; DeSimone, J. M. *Polym. Preprints* **2005**, *46*, 799.

Scheme 1. PFPE-Based Soft Lithography Using Weakly-Adsorbed Particles as Masters<sup>a</sup>

<sup>a</sup> After adsorption of particles on an appropriate substrate, two scenarios are possible. In the first scenario, all of the particles remain adsorbed on the substrate. The resulting PFPE mold can then be used to replicate the master. However, in scenario 2, the particles are lifted off from the substrate and essentially get stuck in the molds. These adhered particles can then be harvested and transferred onto another substrate.

replicate many unique shapes, particularly nonplanar structures, in a variety of sizes which are difficult to obtain from conventional masters.

A vital question when molding soft and weakly adsorbed particles is determining the minimum substrate surface energy in order to reduce particle deformation upon adsorption and yet still be able to successfully replicate these unique and delicate masters. Two scenarios can occur during the molding process (Scheme 1): either the particles remain on the substrate after molding (stronger adhesion to the substrate) or the particles can be removed from the substrate and adhere to the PFPE mold (stronger adhesion to the mold). Stronger adhesion to the substrate enables molding and replication of the particles (scenario 1).<sup>3,12</sup> However, for delicate assemblies such as micelles, one must use low surface energy substrates to minimize particle deformation caused by adsorption, and yet still be able to mold these particles. As such, the range for the substrate surface energies has to be determined in order for molding to be successful. In a similar fashion, the surface energy of each component must be controlled in order to transfer particles between different substrates (scenario 2).<sup>3,13</sup>

In this paper, we report on a PFPE-based soft lithographic method using block-copolymer micelles of poly(styrene)-*b*-poly(isoprene) (PS-*b*-PI) adsorbed on silicon substrates. Block-copolymer micelles provide a flexible model system as one can prepare nanometer sized particles of various shapes (spheres, cylinders, torroids, and vesicles) and sizes ranging from 10 to 1000 nm. In addition, all micelles prepared in the same selective solvent have the same surface composition, which is vital for this study as one wants to maintain the same adhesion while changing the micelle geometry. Micelle dimensions were characterized by light scattering, while the molding steps were monitored using Atomic Force Microscopy (AFM). To examine the effect of particle adhesion to the substrate, the molding process was studied using substrates with systematically varied surface energies. A surface energy threshold before particle removal from the substrate and into the mold was determined. This was in agreement with the theoretical prediction of the molding range, which determines both the minimal surface energy of the substrate and the adsorption-caused particle deformation.

### Materials and Methods

Photocurable perfluoroether (PFPE) films were prepared by UV-cross-linking under an inert atmosphere for 20 min ( $\lambda = 365$  nm,

35 mW/cm<sup>2</sup>), as outlined in a previous publication.<sup>7,8</sup> The surface energy of the cured PFPE films ( $\gamma_{\text{PFPE}} = 16 \pm 4$  mJ/m<sup>2</sup>) was determined from a Zisman plot constructed from contact angle measurements of a homologous series of hydrocarbons (*n*-decane, *n*-dodecane, *n*-tetradecane, and *n*-hexadecane). Contact angle values were obtained using an optical contact angle goniometer from KSV Instruments (CAM 200).

Silicon wafers obtained from Virginia Semiconductor, Inc. were cleaned for 10 min using an ultraviolet-ozone (UVO) cleaner obtained from Jelight Company Inc. (Model 42) before modification. The instrument not only cleans the surfaces but it also introduces -OH functionality on the silicon, which readily reacts with an alkylsilane and produces a hydrocarbon-rich surface. *N*-Octyltrichlorosilane (OTS) and paraffin oil (PO) obtained from Fisher Scientific for substrate modification experiments were used as received. The procedure for modification is described elsewhere.<sup>14,15</sup> After modification, the substrate was cut into strips at specific distances. Each strip was then cut into 2 pieces of approximately 10 × 10 mm. The contact angle was determined for one of the pieces, and the sample was prepared using the second piece. To verify reproducibility, the sample preparation was carried out multiple times followed by contact angle measurements. The contact angle was measured in 3–5 spots along the central line of the 10 × 10 mm<sup>2</sup> area using drops of 1–2 mm in diameter. Milli-Q distilled water ( $\rho = 18.2$  mΩ) was used for the contact angle characterization of the modified substrates.

Block copolymers of PS-*b*-PI with well-defined molecular weights were synthesized by sequential anionic polymerization under high vacuum. Microstructure, chemical composition, and molecular weight distribution, and weight average molecular weights of the prepared polymers were characterized by <sup>1</sup>H NMR, size exclusion chromatography (SEC), and low angle laser light scattering (LALLS). In this paper, we studied diblocks with three different compositions: sample A,  $M_{w,PS} = 39$  kDa,  $M_{w,PI} = 94$  kDa; sample B,  $M_{w,PS} = 39$  kDa,  $M_{w,PI} = 10$  kDa; and sample C,  $M_{w,PS} = 20.6$  kDa,  $M_{w,PI} = 4.3$  kDa. The diblocks have a narrow molecular weight distribution with a polydispersity index of  $M_w/M_n = 1.02$ . The polyisoprene blocks consist of about 93% of *cis*-1,4-polyisoprene.

Diblock solutions were prepared by weighing in filtered *n*-heptane (selective solvent for the polyisoprene block). After being placed under argon, the samples were equilibrated at 60 °C for ~24 h and then slowly cooled to room temperature (~0.1 °C/min). To measure the hydrodynamic radius of the micelles, dynamic light scattering measurements were conducted using a BI-200SM light scattering system equipped with a "TurboCorr" digital correlator for signal processing. Auto correlation functions were measured at three angles (60, 90, 120 degrees) sample. The diffusion coefficient (*D*) was calculated by fitting the correlation curve to a single exponential function for each angle. The hydrodynamic radius (*R<sub>h</sub>*) was then

(12) Gates, B. D.; Whitesides, G. M. *J. Am. Chem. Soc.* **2003**, *125*, 14986–14987.

(13) Loo, Y. -; Willett, R. L.; Baldwin, K. W.; Rogers, J. A. *J. Am. Chem. Soc.* **2002**, *124*, 7654–7655.

(14) Chaudhury, M. K.; Whitesides, G. *Science* **1992**, *256*, 1539–1541.

(15) Efimenko, K.; Genzer, J. *Adv. Mater.* **2001**, *13*, 1560–1563.



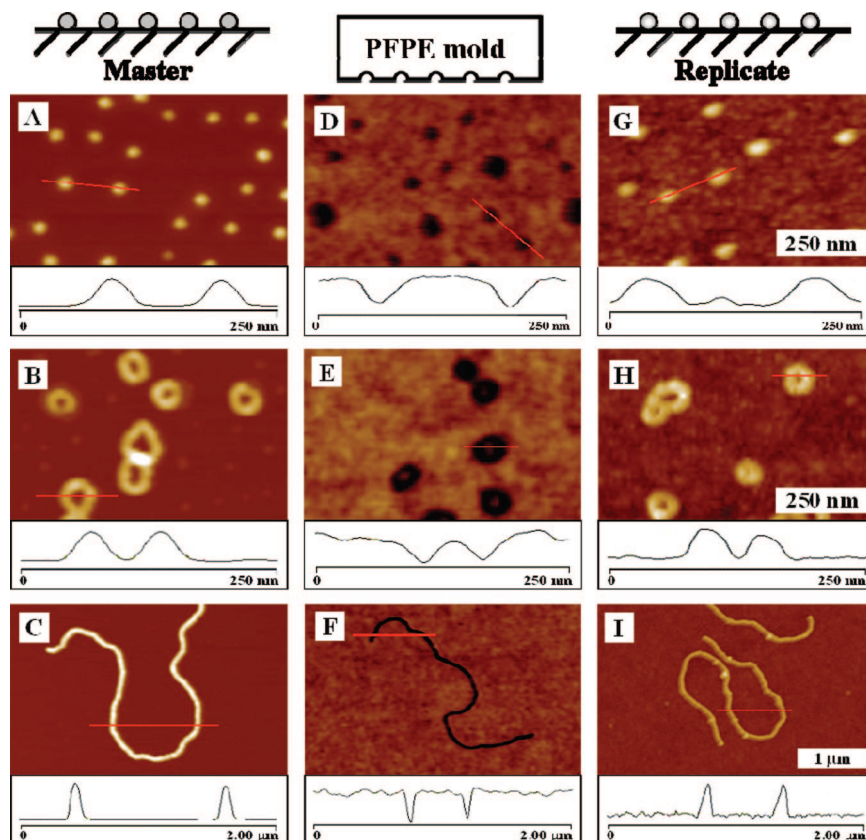


**Figure 1.** PFPE-based soft lithography allows templating and molding of spherical, toroidal, and cylindrical PS-*b*-PI micelles. Figures A–C are the masters of spherical, toroidal, and cylindrical micelles on mica. Figures D–F are the respective PFPE molds. And finally, Figures G–I are the replicas made from the molds using a triacrylate resin. Included are the profiles from each sample, demonstrating the fidelity of the process at each step of the procedure. [Average particle height: spherical master A = 20 nm and replica G = 19 nm; toroidal master B = 12 nm and replica H = 15 nm; cylindrical master C = 26 nm and replica I = 25 nm].

**Table 1. Summary of Results of the Molding Experiments Using Spherical PS-*b*-PI Particles on Modified Silicon Pieces**

substrate	surface energy, $\gamma_1$ (mJ/m <sup>2</sup> )	height (nm)	surface coverage of micelles (# of particles/ $\mu\text{m}^2$ )		
			Before molding	After molding	PFPE mold
substrate A	54	24 $\pm$ 3	8 $\pm$ 2	1.2 $\pm$ 0.2	6 $\pm$ 1
substrate B	57	23 $\pm$ 3	16 $\pm$ 3	15 $\pm$ 3	<1
unmodified silicon wafer	300 (in air)	18 $\pm$ 3	27.2 $\pm$ 0.2	27.4 $\pm$ 0.7	$\sim$ 0

similar to those previously reported (Figure 2b).<sup>15</sup> Thus, the surface modification through vapor diffusion and subsequent chemisorption procedure with the OTS mixture allows for the facile preparation of substrates with broad surface energy  $\gamma$  values ( $\gamma \approx 20$ –100 mJ/m<sup>2</sup>).

**2. Molding of Spherical Micelles.** After characterization, spherical micelles were first spin-cast onto the modified substrates and then taken for molding and replication. Each step was monitored by AFM, which was used to visualize and count particles. Three systems were studied: (1) the substrates with adsorbed particles, that is, the master, (2) the substrates after molding, and (3) the surface structure of the PFPE molds after molding. Table 1 summarizes the results of the experiments.

As a control experiment, PS-*b*-PI spherical micelles were spin-cast onto UVO-cleaned silicon wafers (the surface is -OH functionalized). No particle removal from the substrate was observed, that is, the surface coverage of the particles on bare silicon was constant before and after molding ( $\sim 27$  particles/ $\mu\text{m}^2$ ). However, unmodified silicon wafers caused significant deformation of the particles with a height of 18 nm, which is noticeably below the diameter of the glassy PS core  $D_c = 26 \pm 2$  nm. This was expected because the surface energy of silicon

( $\gamma \approx 300$  mJ/m<sup>2</sup>)<sup>21</sup> is much higher than those for polyisoprene and PFPE.<sup>7,8</sup>

A significant change in the micelle surface coverage was observed on a modified substrate with surface energy of  $\gamma = 50$ –60 mJ/m<sup>2</sup>, that is, there was particle lift-off from the substrate. The transition from no particle removal to lift-off from the substrate was observed in the relatively narrow range of surface energies. Therefore, a more meticulous experiment using modified silicon with  $\gamma_A = 54 \pm 3$  mJ/m<sup>2</sup> (substrate A) and  $\gamma_B = 57 \pm 3$  mJ/m<sup>2</sup> (substrate B) was conducted to narrow down the surface energy range before lift-off occurs. Figure 3A,D show the AFM micrographs of the PS-*b*-PI micelles on substrates A and B, respectively. Even before the molding procedure, it was evident that less particles were adhering to substrate A (8  $\pm$  2 particles/ $\mu\text{m}^2$ ), compared to substrate B (16  $\pm$  3 particles/ $\mu\text{m}^2$ ). This is consistent because  $\gamma_A < \gamma_B$ . The averages and errors associated with the particle density values were determined by measuring the coverage at various areas of the substrates, thus giving a more representative picture for sample.

After initial characterization of the masters, both samples were molded using PFPE, shortly followed by the reexamination of

(21) Messmer, C.; Bilello, J. C. *J. Appl. Phys.* **1981**, *52*, 4623–4629.

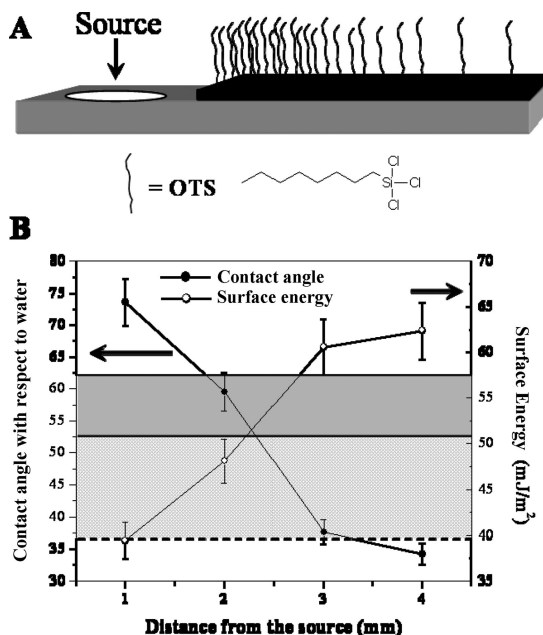


**Figure 2.** Modification of silicon substrates using an alkylsilane mixture. (A) The reaction of the alkylsilane with hydroxyl groups on silicon creates a surface with gradient in surface energy. (B) The contact angle with water and the corresponding surface energy, versus distance graph shows a typical gradient created on OTS-modified silicon substrates. For surface energies above the solid line, adsorbed soft particles are shape deformed but are moldable. The optimal condition for molding soft particles is adsorption at a narrow surface energy threshold (solid gray box). Below this surface energy range, the particles preferentially adhere to the mold, thereby making them ideal for transfer applications (light gray box). And at even lower surface energies (below the dashed line), the particles begin to aggregate, thus losing their shape.

both masters and the surface structure of each mold. As can be seen, there was a dramatic change in substrate **A** after molding, with only  $1.2 \pm 0.2$  particles/ $\mu\text{m}^2$  remaining on the substrate (Figure 3B), while  $6 \pm 1$  particles/ $\mu\text{m}^2$  remained in the mold, that is,  $\sim 80\%$  of the particles lifted-off from the substrate and into the mold was observed (Figure 3C). On the other hand, virtually no change was observed in the particle coverage on substrate **B** after molding ( $15 \pm 3$  particles/ $\mu\text{m}^2$ ; Figure 3E). Note that the images in Figure 3 are a small representation of the collective images taken for each sample. For quantitative comparison, one should use Table 1, which depicts the mean values along with their standard deviations. The obtained results indicate that there is a surface energy threshold required for adsorbed spherical micelles to remain adhered to the substrate for molding and replication, and for our system, that value is  $\gamma \cong 54 \pm 3$  mJ/m<sup>2</sup>.

**3. Calculation of the Surface Energy of Lift-Off: Comparison with Experiment.** A surface energy threshold  $\gamma^*$  for particle lift-off from the substrate can be theoretically estimated based on the following assumptions: (1) due to interaction with the substrate, a soft spherical particle adopts a shape of a hemispherical cap (Figure 4), (2) no further deformation of the particles and PFPE occurs throughout the molding procedure, i.e., the shape of dry micelles with the glassy PS core remain constant, and (3) only dispersion forces are present in the system because the interacting components. The first assumption is verified by the close agreement between the hemisphere volume  $V_{\text{hemisphere}} = (2.5 \pm 1.3) \times 10^4$  nm<sup>3</sup> and the volume of the dry spherical particle,  $V_0 = 4/3\pi \cdot R_{\text{dry}}^3 = (2.9 \pm 1.3) \times 10^4$  nm<sup>3</sup>. The

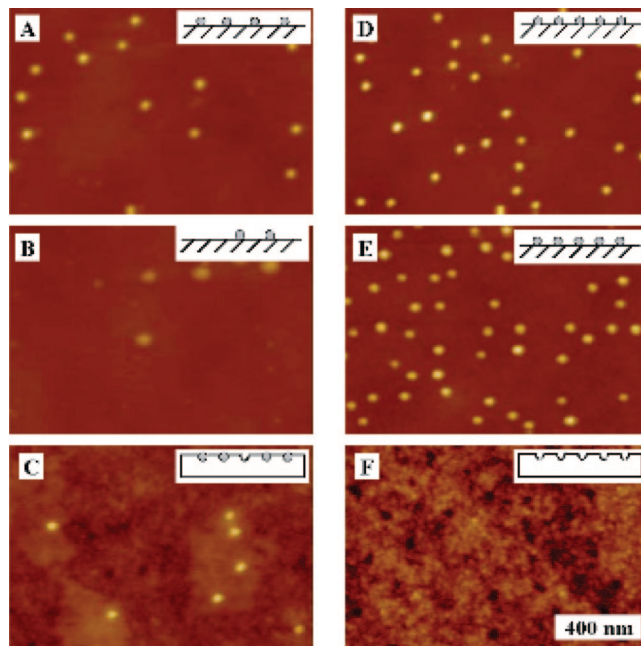


**Figure 3.** AFM images of PS-*b*-PI spherical micelles on two different modified substrates before and after molding, as well as the PFPE molds from each sample. On substrate **A**, there was a significant change in the particle coverage before (A) and after molding (B), that is, there was particle lift-off from the substrate, which was confirmed by the presence of spherical micelles in the PFPE mold (C). On the other hand, for substrate **B**, there was virtually no change in micelle coverage before (D) and after molding (E), which was also confirmed by the mold images (F). The difference in image quality is the result of using several tips with varying tip sharpness.

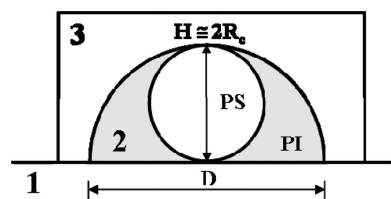


**Figure 4.** Spherical micelle can be approximated as a hemisphere upon adsorption on the substrate, with the height of the cap being the diameter of the PS core [1: modified silicon substrate; 2: PS-*b*-PI micelle; 3: PFPE mold].

second assumption is verified by measuring nearly identical cross-sectional profiles of the master, mold, and replica (Figure 1). The third assumption is consistent with the nonpolar and neutral nature of the studied materials (PI-covered micelles, modified silicon wafers, and the PFPE mold).<sup>22</sup>

As shown in Appendix A, onset of particle lift-off occurs at surface energies of the substrate  $\gamma_1 < \gamma^* \cong (\Sigma_{23} / \Sigma_{12})^2 \cdot \gamma_3$ , where  $\Sigma_{23} \cong \pi \cdot D \cdot H$  is the area of interface between the mold and the micelle and  $\Sigma_{12} \cong \pi D^2 / 4$  is the area of the interface between the micelle and the substrate (Figure 4). The height  $H = 23 \pm 3$  nm was determined directly from the cross-sectional profiles. The diameter of the adsorbed micelles  $D = 45 \pm 5$  nm was determined from length measurements between contiguous micelles and subsequent extrapolation of the linear fit to the y-intercept (single micelle) to reduce the effect of tip shape.<sup>16,17</sup> Therefore, for the studied system ( $\Sigma_{23} / \Sigma_{12} \cong 2.0 \pm 0.3$ ,  $\gamma_2 = 30$  mJ/m<sup>2</sup>,<sup>23</sup> and  $\gamma_3 = 14$  mJ/m<sup>2</sup>), one finds that particle lift-off from the substrate onto the PFPE molds should occur at an average substrate surface

(22) Israelachvili, J. *Intermolecular and Surface Forces*; Academic Press: San Diego, 1992; p 450.

(23) Wu, S. *Polymer Handbook*; John Wiley & Sons, Inc.: New York, 1999; Chapter 6.

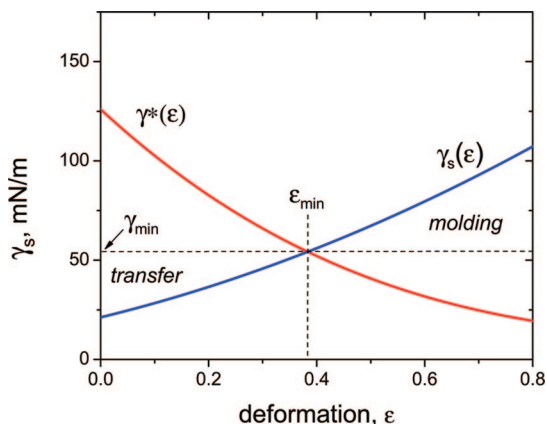


**Figure 5.** Diagram of the molding and transfer conditions for a rubber-like particle with thickness  $H_0 = 25$  nm, Young's modulus  $E = 1$  MPa, asymmetry ratio  $\alpha = 2$ , and  $\gamma_p = 30$  mJ/m<sup>2</sup>. Molding and replication of this particle is allowed if the surface energy of the substrate is larger than the threshold surface energy for particle lift-off  $\gamma_s > \gamma_s^*(\epsilon)$ , while the transfer is possible at  $\gamma_s < \gamma_s^*(\epsilon)$ . The minimal deformation  $\epsilon_{\min} \cong 0.38$  (i.e., 38%) of the particle upon molding is achieved at  $\gamma_s = \gamma_{\min}$ .

energy of  $\gamma^* = 56 \pm 7$  mJ/m<sup>2</sup>. This is in agreement with the empirically determined lift-off range of  $\gamma_1 \cong 54\text{--}57$  mJ/m<sup>2</sup>. At surface energies higher than 54 mJ/m<sup>2</sup>, the master can be used for molding and replication, but the particles undergo deformation due to attraction to the substrate. Thus, depending on the application, one can set an upper tolerance limit  $\gamma_{\max}$  for the deformation, which will determine the molding range  $\gamma^*/\gamma_{\max}$  (discussed below). At energies below the  $54 \pm 3$  mJ/m<sup>2</sup> threshold, the particles were lifted-off from the substrate and into the mold, that is, each individual particle is harvested into the mold. The mold containing the harvested spheres can then be transferred and used in other applications. However, at lower surface energies,  $\sim 40$  mJ/m<sup>2</sup>, the individual spheres underwent ill-defined aggregation. This sets a lower limit of the substrate surface energy for particle harvesting and transfer applications. The surface energy ranges for molding and transfer applications are highlighted in Figure 2 by solid gray and light gray boxes, respectively.

The above calculations were performed for a fixed particle shape and given surface energies. However, when dealing with soft nanoparticles, the effect of interfacial interactions is more complex, as it changes both particle adhesion and particle shape, that is, contact areas. By increasing the surface energy of the substrate, one increases the particle-substrate adhesion, which also decreases the contact area with the mold. Both factors promote molding, however, this occurs at the expense of particle deformation which may hinder certain molding applications, especially those involving small ( $R \sim 10$  nm), soft particles ( $E \sim 1$  MPa) with surface energy  $\gamma_p \sim 10$  mJ/m<sup>2</sup>. As such, for every type of master (size, shape, and stiffness), one has to determine the lift-off threshold ( $\gamma_{\min} = \gamma^*$ ) and the minimal particle deformation ( $\epsilon_{\min}$ ). The details of calculations are presented in Appendices B and C. The calculations were conducted for a simple shape of square cuboid and can be generalized for any particle shape. Figure 5 shows plots of eqns C.1 and C.2 from Appendix C, which depict the molding threshold  $\gamma^*$  and the actual substrate surface energy  $\gamma_s$  as a function of the particle deformation  $\epsilon$ . The plots were calculated for a square cuboid with height  $H_0 = 25$  nm, Young's modulus  $E = 1$  MPa, asymmetry parameter  $\alpha = 2$ , and particle surface energy  $\gamma_p = 30$  mJ/m<sup>2</sup>. The choice of parameters mimics the properties of adsorbed spherical micelles. Figure 5 shows that the molding can be performed in the range of the surface energies  $\gamma_s(\epsilon) > \gamma_{\min} =$

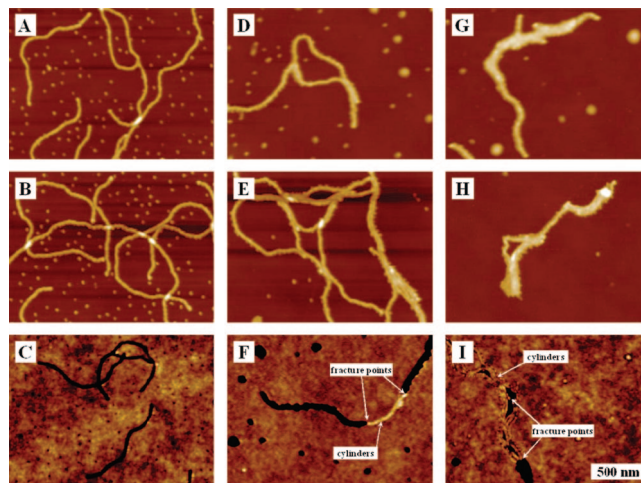


**Figure 6.** AFM images of PS-*b*-PI cylindrical micelles on modified silicon substrates. Similar to the spheres, no lift-off from the substrate was observed before (A) and after (B) molding of cylindrical micelles on a substrate with high surface energy (mold image C). On substrates with lower surface energy, partial (D: master before molding; E: master after molding) to extensive (G: master before molding; H: master after molding) lift-off of the cylinders from the substrate were detected upon imaging the molds (F and I, respectively). Complete removal of the cylinders from the substrate has not been observed at this time.

55 mJ/m<sup>2</sup> for finite deformations of the master particles with  $\epsilon > 0.38$ . This range of parameters is consistent with the experimentally determined molding threshold  $\gamma_1 \cong 54\text{--}57$  mJ/m<sup>2</sup>.

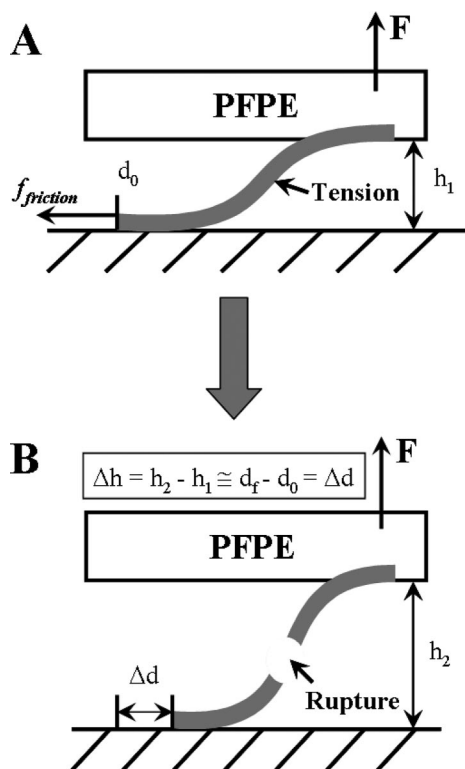
**4. Molding of Cylindrical Micelles.** To investigate the effect of particle geometry on the adhesion, and its effect on the critical surface energy before particle lift-off from the substrate, preliminary experiments were conducted using cylindrical PS-*b*-PI ( $M_{PS} = 40$  kDa,  $M_{PI} = 10$  kDa). It is important to reiterate that the chemical structure of the cylinders is identical to that of the spherical micelles and that only the ratio of the blocks is different, which causes the change in micelle morphology. In using these molecules, one minimizes the effects from the chemical interactions between the various components of the system.

A solution containing both spheres and cylinders was spin-cast onto modified silicon substrates. The spherical micelles were used as surface energy gauges for this preliminary test. As discussed previously, the adsorbed spheres are known to lift-off at  $\gamma \cong 54$  mJ/m<sup>2</sup>. Slightly below this threshold, the spheres are lifted-off of the substrate and into the mold, while at surface energies significantly lower than 54 mJ/m<sup>2</sup>,  $\sim 40$  mJ/m<sup>2</sup>, the spherical micelles undergo aggregation.

On the substrate with the high surface energy ( $\gamma > 54$  mJ/m<sup>2</sup>), the cylinders behaved similar to their spherical counterparts, that is, they remained on the surface and no lift-off of the particles into the mold was observed (Figure 6A–C). However, in contrast to the complete lift-off of the spheres, weakly adsorbed cylinders ruptured at surface energies just below  $\gamma < 54$  mJ/m<sup>2</sup> (Figure 6D), leaving behind portions of the molecule on the substrate (Figure 6E) and in the mold (Figure 6F). And at an even lower surface energy ( $\gamma \ll 54$  mJ/m<sup>2</sup>) (Figure 6G), a large fraction of cylindrical micelles adhered to the mold (Figure 6I) but some sections remained on the substrate (Figure 6H).

The presence of torn cylinders can be explained by the fact that removal of extended objects from a substrate by lift-off involves their sliding, which is hindered by micelle sections adsorbed to the substrate (Scheme 3A). The cylinder under tension

**Scheme 3. Molding of Cylindrical Micelles Using Low Energy Substrates Results in Micelle Rupture upon Mold Removal<sup>a</sup>**



<sup>a</sup> (A) During mold removal, parts of the cylinder are unable to slide on the surface and essentially pinned on the surface as the friction force ( $f_{\text{friction}}$ ) is quite strong. This creates tension within the molecule; (B) and as the mold is further lifted up from the master, the cylinder ruptures when the force of friction exceeds the cohesive forces keeping the micelle intact ( $f_{\text{cohesion}}$ ).

ultimately breaks when the friction force  $f_{\text{friction}}$  becomes greater than the cross-sectional cohesive forces in the micelle (Scheme 3B). Given that the frictional force acting on the cylinder is  $f_{\text{friction}} \sim l \cdot r$ , while the cohesive forces in the micelle is only  $f_{\text{cohesion}} \sim r^2$ , with  $l \sim 1\text{--}10 \mu\text{m}$  and  $r \sim 10 \text{ nm}$ , it is easy to see why the fracture of the cylinder is very likely to occur in these circumstances. This demonstrates the essential difference in the application of soft lithography for spherical and cylindrical objects. While molding of spherical micelles should be performed at the surface energy threshold to minimize deformation to the soft particle, cylindrical assemblies must be molded at higher surface energies to prevent rupture of the cylinder. This, however, assumes larger deformation of the master particles.

### Conclusions

In conclusion, the molding of spherical and cylindrical PS-*b*-PI block-copolymer micelles using PFPE on substrates of different surface energies was successfully studied by AFM. It was found that particle geometry had a significant impact on the adhesion and the substrate surface energy wherein molding of the particles should be carried out. A surface energy threshold,  $\gamma \cong 54 \text{ mJ/m}^2$ , was determined for the weakly adsorbed spherical micelles to be lifted-off from the substrate and into the mold. In the case of cylindrical micelles, fracture was observed instead of the expected micelle lift-off at surface energies lower than that determined for their spherical counterparts ( $\gamma < 54 \text{ mJ/m}^2$ ). This observation is ascribed to the inability of the adsorbed cylinder sections to slide on the surfaces during mold removal. This illustrates a significant procedural difference in molding

spherical and cylindrical objects. The balance between minimization of particle deformation and lift-off from the substrate requires that soft spheres be molded at the surface energy threshold, while cylindrical assemblies must be molded at higher surface energies, at the cost of some shape distortion, to prevent breakage of the object. One can circumvent rupture of long and fragile objects like the cylindrical micelles during molding by either using substrates with higher surface energies than that determined for the spherical particles, or using stronger particles, such as carbon nanotubes, as masters.<sup>18</sup>

The existence of a surface energy threshold for particle adhesion and removal from the substrate has been verified theoretically. The calculations predicted a surface-energy range that allows molding and replication of soft nanoparticles at a minimal deformation. The range strongly depends on the particle size, shape, and mechanical properties. As shown in Appendix C, the adsorption-induced deformation is only significant for soft nanometer-sized particles with  $EH < 1000 \text{ mN/m}$ , for example,  $E < 10 \text{ MPa}$  and  $H < 100 \text{ nm}$ . For larger and stiffer particles with  $EH > 1000 \text{ mN/m}$ , the adsorption induced deformation may be neglected. The molding also depends on the surface energy of the particle and mold precursor. Therefore, the exact location of the threshold needs to be determined for each molding system to be explored.

**Acknowledgment.** We thank Dr. Ashish Pandya for providing PFPE precursors and all members of Prof. DeSimone's group for allowing the use of their equipment. We also thank Dr. Kirill Efimenko and Prof. Jan Genzer of NC State University for their help with substrate modifications. This work was funded by the National Science Foundation (DMR-0606086 and STC CHE-9876674), Liquidia Technologies (SRA P no. 07-1820), and Defense Advanced Research Projects Agency (W911NF-06-1-0343).

### Appendix A: Onset of Lift-Off

During the lift-off process, an external force is applied to separate a master particle from either the master mold or the substrate. The first scenario is desirable for particle replication (Scheme 1, scenario 1), while the second scenario is favored for harvesting and subsequent transfer of particles for various applications (Scheme 1, scenario 2). The work against adhesion will be smaller when creating the new interfaces with lower surface energies. Here we assume that particles are hard and the lift-off process is faster than the particle relaxation times. For the relatively large particles ( $H > 10 \text{ nm}$ ), we also neglect the contribution of the long-range van der Waals forces. Under these assumptions, one can write the following expressions for the total interfacial free energy created during the lift-off process corresponding to scenarios 1 and 2, respectively:

$$F_1 = (A_{\text{tot}} - \Sigma_{\text{sp}})\gamma_s + \Sigma_{\text{pm}}\gamma_p + \Sigma_{\text{sp}}\gamma_{\text{sp}} + (A_{\text{tot}} - \Sigma_{\text{sp}} + \Sigma_{\text{pm}})\gamma_m \quad (\text{A.1})$$

$$F_2 = A_{\text{tot}}\gamma_s + \Sigma_{\text{pm}}\gamma_{\text{pm}} + \Sigma_{\text{sp}}\gamma_p + (A_{\text{tot}} - \Sigma_{\text{sp}})\gamma_m$$

where  $A_{\text{tot}}$  is the surface area of the substrate per adsorbed particle,  $\Sigma_{\text{sp}}$  and  $\Sigma_{\text{pm}}$  are the areas of the substrate-particle and particle-mold interfaces;  $\gamma_s$ ,  $\gamma_p$ , and  $\gamma_m$  are the surface energies of the substrate, polymer, and mold;  $\gamma_{\text{pm}}$  and  $\gamma_{\text{sp}}$  are the interfacial energies of particle-mold and substrate-particle interfaces, respectively. Thus, the master will separate from the mold if

$$F_2 - F_1 = \Sigma_{\text{pm}}(\gamma_{\text{pm}} - \gamma_p - \gamma_m) + \Sigma_{\text{sp}}(\gamma_p + \gamma_s - \gamma_{\text{sp}}) > 0 \quad (\text{A.2})$$

When the Good-Girifalco relation is used,  $\gamma_{12} = \gamma_1 + \gamma_2 - 2\sqrt{\gamma_1\gamma_2}$  for the interfacial energy between phases 1 and 2 in

terms of their surface energies, one can rewrite the lift-off condition as follows

$$\sqrt{\gamma_s} > \frac{\sum_{\text{pm}} \sqrt{\gamma_m}}{\sum_{\text{sp}}} \quad (\text{A.3})$$

In other words, the threshold surface energy for successful molding is

$$\gamma^* = \left( \frac{\sum_{\text{pm}}}{\sum_{\text{sp}}} \right)^2 \gamma_m \quad (\text{A.4})$$

At surface energies  $\gamma_s > \gamma^*$ , particles remain adsorbed to the substrate (scenario 1). For lower surface energies ( $\gamma_s < \gamma^*$ ), the particles will be lifted-off from the substrate and remain embedded into the mold (scenario 2).

### Appendix B: Master Deformation

Adsorption to a substrate causes deformation of master particles. Let us consider the deformation of a particle having a shape of square cuboid prior to lift-off (Figure 7). The undeformed cuboid has height  $H_0$ , length  $L_0 = \alpha H_0$ , and the area of the square bottom face  $\Sigma_0 = L_0 \times L_0$ . Upon deformation, the height of the cube decreases as

$$H = (1 - \varepsilon)H_0 \quad (\text{B.1})$$

In the case of a rubber-like particle, it deforms at a constant volume such that the areas of the top and bottom facets increase with deformation as

$$\Sigma = L_0^2(1 - \varepsilon)^{-1} \quad (\text{B.2})$$

Adsorption-induced deformation is calculated from the balance of the interfacial ( $F_{\text{surf}}$ ) and elastic ( $F_{\text{elast}}$ ) free energies that have the following expressions (assuming small deformations  $\varepsilon < 1$ ):

$$F_{\text{surf}} = (A_{\text{tot}} - \Sigma)\gamma_{\text{sl}} + (\gamma_{\text{pl}} + \gamma_{\text{sp}})\Sigma + 4\gamma_{\text{pl}}\sqrt{\Sigma}R_d \approx A_{\text{tot}}\gamma_{\text{sl}} - (S\alpha - 4\gamma_{\text{pl}})\alpha H_0^2 - (S\alpha + 2\gamma_{\text{pl}})\alpha H_0^2\varepsilon \quad (\text{B.3})$$

$$F_{\text{elast}} = \frac{EV}{6}(2(1 - \varepsilon)^{-1} + (1 - \varepsilon)^2 - 3) \approx \frac{E\alpha^2 H_0^3}{2}\varepsilon^2 \quad (\text{B.4})$$

where  $E$  is the Young's modulus of the particle,  $\alpha$  is the asymmetry parameter, and  $S$  is the spreading parameter. Here the liquid phase ( $l$ ) is referred to as the precursor for the mold. Combining together surface and elastic energies and keeping only  $\varepsilon$  dependent parts, one obtains the following expression for the increment of the free energy due to the deformation of the adsorbed cubes

$$\Delta F(\varepsilon) \approx -(S\alpha + 2\gamma_{\text{pl}})\alpha H_0^2\varepsilon + \frac{E\alpha^2 H_0^3}{2}\varepsilon^2 \quad (\text{B.5})$$

The optimal value of the cube deformation, which optimizes both the surface energy and the elastic energy contributions, is

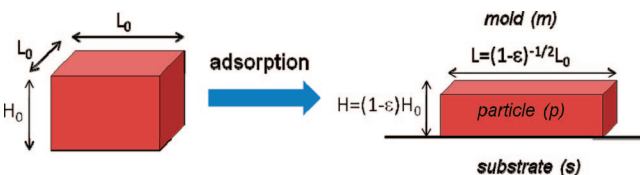


**Figure 7.** Deformation of a cuboid ( $L_0 \times L_0 \times H_0$ ) upon adsorption to a substrate.

obtained by minimizing the free energy with respect to deformation  $\varepsilon$

$$\varepsilon \approx \frac{(S\alpha + 2\gamma_{\text{pl}})\alpha H_0^2}{E\alpha^2 H_0^3} = \frac{1}{EH_0} \left( S + \frac{2\gamma_{\text{pl}}}{\alpha} \right) \quad (\text{B.6})$$

where the spreading parameter  $S$  and the polymer–liquid interfacial energy can be written as follows

$$S \approx 2(\sqrt{\gamma_p} - \sqrt{\gamma_l})(\sqrt{\gamma_s} - \sqrt{\gamma_p}) \quad (\text{B.7})$$

$$\gamma_{\text{pl}} \approx (\sqrt{\gamma_p} - \sqrt{\gamma_l})^2 \quad (\text{B.8})$$

Thus, there is a very simple relationship between the deformation and the system parameters, which leads to the following conclusions: (1) The deformation is inversely proportional to the Young's modulus (harder samples are more difficult to deform). (2) The deformation increases as the surface energies of the particle-liquid and substrate-liquid interfaces increase (the deformation of the sample leads to decrease of the particle-liquid contact area and to increase of the particle-substrate area). (3) The deformation is also inversely proportional to the size of the cube, which indicates that one will need a larger Young's modulus to achieve the same quality of the mold for reproduction of the smaller features.

### Appendix C: Optimal Conditions for Molding

Let us analyze conditions for optimal molding by calculating a molding range confined between the minimal deformation (under given conditions  $E$ ,  $H_0$ ,  $\gamma_m$ , and  $\gamma_p$ ) and allowable deformation (tolerance). For this purpose, we write two conditions: (i) for the minimal deformation at the lift-off onset (eq A.4) and (ii) deformation at a given surface energy of the substrate  $\gamma_p$  (Eq. B.6). These conditions can be presented in terms of  $\varepsilon$  and  $\gamma_s$  as follows:

$$\gamma_s \geq \gamma^*(\varepsilon) = \left( \frac{\sum_{\text{pl}}}{\sum_{\text{sp}}} \right)^2 \gamma_m = \left( 1 + \frac{4\sqrt{1 - \varepsilon}H_0L_0}{(1 - \varepsilon)^{-1}L_0^2} \right)^2 \gamma_m = \left( 1 + \frac{4}{\alpha}(1 - \varepsilon)^{3/2} \right)^2 \gamma_m \quad (\text{C.1})$$

$$\varepsilon \geq \frac{2}{EH_0}(\sqrt{\gamma_p} - \sqrt{\gamma_m})(\sqrt{\gamma_s} - \sqrt{\gamma_p} + \frac{1}{\alpha}(\sqrt{\gamma_p} - \sqrt{\gamma_m})) \quad (\text{C.2})$$

It is important to point out that the particle molding is successful only within the range of the defined parameters, where both conditions are satisfied.

The intersection of equations C.1 and C.2 gives the minimal particle deformation  $\varepsilon_{\text{min}}$  and the threshold surface energy of the substrate  $\gamma_{\text{min}}$ . In Figure 8, we plot the dependence of  $\varepsilon_{\text{min}}$  and  $\gamma_{\text{min}}$  (see Figure 5) as a function of the parameter  $EH$  (effective stiffness) for two types of mold materials (PFPE and PDMS). As expected, the minimal allowable deformation  $\varepsilon_{\text{min}}$  decreases with increasing the particle stiffness (modulus  $\times$  size; Figure 8a). The opposite behavior is demonstrated by the minimal surface energy of the substrate  $\gamma_{\text{min}}$ , which increases with the particle stiffness (Figure 8b). This indicates that molding of larger and stiffer particles requires higher energy substrates, whereas smaller and softer particles can be molded at lower surface energies, but they undergo larger deformation. Important and counterintuitive conclusions are drawn when comparing the PFPE and PDMS molds. On one hand, the minimal particle deformation is lower for the PDMS mold due to the smaller value of the spreading parameter. On the other hand, this advantage cannot be harnessed because molding with PDMS requires substrates with much higher

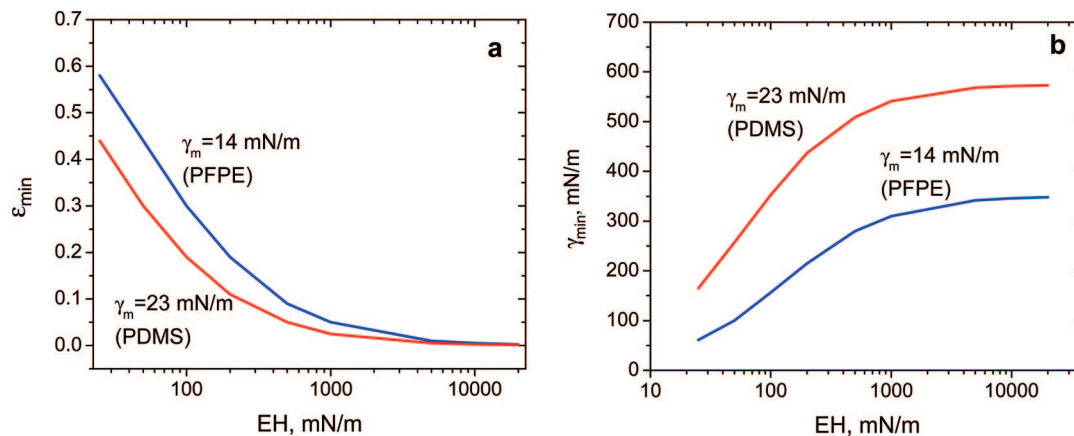


**Figure 8.** Diagrams for the dependence of the minimal deformation of particles (a) and (b) threshold surface energy of the substrate (b; both calculated at the molding threshold depicted in Figure 5) on the effective stiffness of the particles. The calculations were done for molding by PDMS and PFPE resins of particles with  $\gamma_p = 30$  mJ/m<sup>2</sup>.

surface energies ( $\gamma_s > 200$  mJ/m<sup>2</sup>), making preparation of the master nearly impossible. Adsorption of soft nanoparticles on high energy substrates may lead to significant deformation and irrecoverable damage of the supramolecular assemblies such as micelles. In addition, molding organic particles using PDMS involves swelling of the particles with the PDMS molecules,

which also enhances the particle deformation. Unlike PDMS, the semifluorinated PFPE is not miscible with organic materials, thus ensuring a sharp interface between the mold and the particle.

LA802549S